2024 IEEE International Conference on Robotics and Automation (ICRA 2024)
May 13-17, 2024. Yokohama, Japan

Sense in Motion with Belief Clustering: Efficient Gas Source Localization with Mobile Robots

Wanting Jin and Alcherio Martinoli

***Abstract*— Given the patchy nature of gas plumes and the slow response of conventional gas sensors, the use of mobile robots for Gas Source Localization (GSL) tasks presents significant challenges. These aspects increase the difficulties in obtaining gas measurements, encompassing both qualitative and quantitative aspects. Most existing model-based GSL algorithms rely on lengthy stops at each sampling point to ensure accurate gas measurements. However, this approach not only prolongs the time required for a single measurement but also hinders sampling during robot motion, thus exacerbating the scarcity of available gas measurements. In this work, our goal is to push the boundaries in terms of continuity in sampling to enhance system efficiency. Firstly, we decouple and comprehensively evaluate the impact of both plume dynamics and gas sensor properties on the GSL performance. Secondly, we demonstrate that adopting a continuous sampling strategy, which has been generally overlooked in prior research, markedly enhances the system efficiency by obviating the prolonged measurement pauses and leveraging all the data gathered during the robot motion. Thirdly, we further expand the capabilities of the continuous sampling by introducing a novel informative path-planning strategy, which takes into account all the information gathered along the robot's movement. The proposed method is evaluated in both simulation and reality under different scenarios emulating indoor environmental conditions.**

I. Introduction

Determining the source of a gaseous chemical leak released into the air has numerous applications in various critical situations [1]. In recent years, the area of Mobile Robotic Olfaction (MRO) has experienced tremendous growth. Despite such increased attention, a number of challenges related to gas sensing techniques and gas dispersion modeling remain unsolved, thereby impeding their application in real-world scenarios. Gas dispersion is a complex phenomenon that combines advection due to airflow, turbulent diffusion, as well as molecular diffusion [2]. Consequently, the gas plume exhibits intermittent and chaotic characteristics [3], whereby the gas concentration at any given point in the plume demonstrates dynamic and fluctuating behavior, as shown in Fig.1a. This dynamic behavior makes the inference of the source location from gas measurements a challenging task. Additionally, while executing a GSL task within realistic scenarios, obstacles in the environment introduce additional turbulence in the airflow [4]. Furthermore, the

The authors are with the Distributed Intelligent Systems and Algorithms Laboratory, School of Architecture, Civil and Environmental Engineering, École Polytechnique Fédérale de Lausanne (EPFL), 1015 Lausanne, Switzerland. This work was partially funded by the Swiss National Science Foundation under grant 200020_175809. Additional information about the research can be found here: https://www.epfl.ch/labs/disal/research/gassensingstructure/

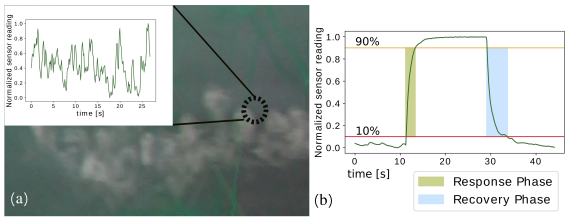

Fig. 1: (a) Evolution of gas concentration measured by a static sensor in a plume; (b) Dynamics of a MOX gas sensor when exposed to a sudden change in gas concentration (air-gas-air experiment in a controlled gas chamber).

predominantly employed gas sensor in MRO, the Metal-Oxide (MOX) sensor, can only provide highly localized measurements of the gas concentration, with non-negligible response and recovery times [5], as shown in Fig.1b. As a result, when monitoring gas concentration in a plume with MOX sensors, the gas measurements are not only noisy because of the patchiness of the plume but also distorted in time due to the intrinsic dynamics of the sensor.

GSL algorithms can be classified into model-free and model-based algorithms. Model-free refer to algorithms that use statistical features of local gas patches, such as gas detection events [6], gas gradient direction [7], or the frequency of gas hits [8], to guide robot movements. These methods rely on the magnitude differences between gas readings rather than on their absolute value. While model-free algorithms are characterized by a low computational cost, they are typically too fragile to cope with complex environments [9]. Model-based algorithms infer the source position efficiently from scattered measurements and make informative navigation decisions by incorporating knowledge of gas dispersion models [10]. The belief of a candidate source position is updated by comparing the actual measurements and the expected concentrations derived from the plume model. As a result, the accuracy of the absolute value of the measurement is essential for the convergence of the estimation process [11]. Therefore, while a strategy relying on continuous gas sampling, which we will call *sense-in-motion* in this paper, is widely used in model-free algorithms, a strategy that involves lengthy stops, which we will call *stop-sense-go* in this paper, is typically employed in model-based algorithms. In the latter strategy, a stopping window of several seconds is employed [12]–[17], and the average reading is considered as a single measurement, given the previously discussed noisy nature of gas measurements. In [18], the effect of both sensor response time and duration of the stop-and-measure phase on a model-based GSL method is studied. The authors concluded that a

lengthy stop at each sampling point is essential for achieving an accurate localization outcome. However, the *stop-sense-go* strategy presents several limitations: firstly, it is time-consuming and, therefore, not suitable for emergency applications. Secondly, it fails to include measurements obtained while moving, which can yield significant insights despite their inherent noise. Thirdly, as measurements are only taken at the sampling locations, the informative goal selection is critical to the overall success. Lastly, when deploying rotary-wing aircraft for GSL tasks, hovering at the sampling point can potentially lead to the dilution of the gas concentration in the area due to the down-wash effect [19] [20].

Several studies explored the potential benefit and impact of continuous sampling on the gas sensing quality. In [21], the impact of the robot's speeds on continuous sampling is studied, where a negative correlation between the sensor response amplitudes and the robot speed is indicated. The study conducted in [22] shows that when there is no continuous airflow, driving the robot with a constant speed introduces an extra constant airflow to the sensor, which improves its sensitivity compared to the *stop-sense-go* strategy. In [23], the gas readings derived from a gas distribution map, created through continuous measurements in motion, are used for GSL tasks carried out in an obstacle-free environment. However, it is unclear whether the good performance of the *sense-in-motion* approach is due primarily to the usage of a kernel-based interpolation technique for gas mapping [24] and can be maintained in more complex environments. Despite the numerous advantages of a continuous sampling method, its integration into model-based GSL algorithms has received limited attention so far.

Informative Path Planning (IPP) is commonly used in probabilistic GSL frameworks [25] to maximize the information gain at the next sampling point to increase the efficiency of the algorithm. The information gain can be defined as a measure of relative entropy, such as entropy loss [26] or the Kullback-Leibler Divergence (KLD) [27] [28]. However, this type of IPP exhibits two limitations. Firstly, these algorithms usually require the prediction of gas measurements at candidate sampling locations, which are not always trivial to obtain. Secondly, the calculation of the updated posterior for each candidate location is required, leading to additional computational cost as the number of locations increases [29]. As a result, previous contributions typically constrained the number of possible candidate locations to a limited set. In the context of continuous sampling, the traditional computationally intensive assessment of information solely at a limited number of locations proved to be less competitive.

This study aims at filling the research gap mentioned above by quantitatively investigating the impact of the **plume dynamics** and the **sensor properties** on GSL model-based probabilistic approaches. In addition, it aims at devising a dedicated IPP method able to take advantage of a *sensing-in-motion* strategy. More concretely, this paper has the following contributions:

- Section II-A elaborates on the design of dedicated experiments to verify the viability and efficiency of a *sense-in-motion* strategy in a Source Term Estimation (STE) algorithm, serving as an example of model-based probabilistic approaches for GSL;
- Section II-C introduces a novel belief-clustering-based path planning algorithm, enabling efficient scanning of the informative regions using an underlying *sense-in-motion* approach;
- Sections III and IV perform a thorough evaluation and result analysis of the proposed algorithm, using high-fidelity simulation and physical experiments, respectively.

II. Methodology

In this section, we define various gas sensor models and sampling strategies, introduce the STE algorithm, and then present both the commonly adopted and our novel IPP methods.

A. Gas Sensor Models and Sampling Strategies

Based on literature contributions, the main rationale in favor of a *stop-sense-go* strategy can be summarized as:

Argument I*: The gas dispersion models used in STE algorithms are usually time-averaged models [3].* To establish alignment between actual gas measurements and those predicted by a plume model, it is, in principle, necessary to stop for a specific duration and use the mean values as measured data.

Argument II*: MOX sensors have a slow reaction and recovery time [30].* Consequently, a *stop-sense-go* strategy enables MOX sensors to effectively react to gas stimulus with prolonged sampling durations, providing more accurate readings.

To quantitatively and separately evaluate the impact of the two arguments above on the performance of STE algorithms, leveraging high-fidelity simulation, we have designed an experimental campaign involving idealized and realistic gas sensors and different sampling strategies as follows.

1) Gas sensors:

- ***Ideal*** gas sensor: negligible response and recovery time, considered as the ground truth for gas concentration.
- ***MOX*** gas sensor: non-negligible response and recovery time, calibrated on the deployed physical sensor.

2) Sampling strategies:

- ***Stop-sense-go***: uses the average gas reading over 5 s at each sampling point.
- ***Visit-sense-go***: uses the instantaneous gas reading at each sampling point.
- ***Sense-in-motion***: uses instantaneous gas readings, both at each sampling point and during the robot's motion.

B. Source Term Estimation Algorithm

STE is a well-known inverse modeling algorithm for GSL tasks able to estimate the source terms, such as the gas source location, release rate, and wind speed [25]. It leverages a steady-state plume model and gas measurements gathered at different sampling positions to update the Probabilistic Distribution Function (PDF) of estimated

source terms iteratively. At each iteration k, the likelihood $p(D_{1:k}|\mathbf{\Theta})$, representing the probability of gathering a series of measurements $D_{1:k} = \{d_1...d_k\}$, given a set of source terms $\mathbf{\Theta}$, is calculated through the difference between the concentration value c_k predicted by the plume model, and the measurement d_k at kth sampling point. σ_M and σ_D stand for standard deviations of model and measurement errors, respectively.

$$p(D_{1:k}|\mathbf{\Theta}) \propto exp\Big(-\frac{1}{2}\sum_{k=0}^{N}\frac{(d_k - c_k(\mathbf{\Theta}))^2}{\sigma_M^2 + \sigma_D^2}\Big) \quad (1)$$

Bayesian inference is used to update the posterior PDF $p\left(\mathbf{\Theta} \mid D_{1:k+1}\right)$, representing the probability of the source term being the set $\mathbf{\Theta}$ when a new measurement d_{k+1} is available. We consider the evidence $p(D_{1:k})$ to be a normalization factor and the prior $p(\mathbf{\Theta})$ a uniform distribution within each parameter limits. The process stops when either the maximum number of iterations is reached or the entropy of the PDF, which measures the estimation uncertainty, drops below a predetermined threshold. In our work, the estimated source terms are the gas source location, namely $\mathbf{\Theta} = \{S_x, S_y\}$. The STE algorithm has been extensively evaluated in obstacle-free environments under consistent wind conditions [31] [28]. Such scenarios are selected to ensure the assumptions of the analytical gas dispersion model, such as the Gaussian Plume Model (GPM), are satisfied. In our previous work [32], we extended the STE algorithm to built environments by replacing the analytical plume model with a Data-Driven Plume Model (DDPM), which is trained with gas dispersion maps under environments with different obstacle configurations. In this work, to validate the generality of the proposed approach, we test our system by deploying the same STE algorithm with both GPM and DDPM.

C. Informative Path Planning

IPP is used to improve the navigation efficiency of the robot, in particular by reducing the time needed for completing a GSL task. There are multiple possible implementations for IPP-based navigation.

1) IPP Based on Kullback-Leibler Divergence [14]: a navigation vector that incorporates a weighted sum of exploration and exploitation factors is employed for the goal selection. The exploratory component considers a set of most informative goals by assessing maneuvers in eight ordinal directions with a predefined step length. The evaluation of the information gain is based on KLD [33] between the current and updated PDFs after sampling at each candidate goal. The exploitative component points to the most likely location of the source.

2) IPP Based on Belief Clustering: a novel IPP method tailored for *sense-in-motion* strategy. Compared to the KLD-based IPP, which evaluates the information gained solely at goal positions (end of the path), our approach evaluates the navigation goals by taking into account information gathered along the entire path.

a. Dynamic clustering of the belief - While sampling in motion, the efficiency of the information gathering can be improved by directing attention toward critical areas rather than isolated critical points. Hence, it is important to categorize the informative cells into coherent regions and prioritize the visit of these regions. We use a dynamic threshold to identify cells with significant information. Next, a density-based clustering algorithm, DBscan [34], is utilized to cluster the identified cells. The resulting clusters will be the connected cells with sufficient information. The IPP algorithm is altered to prioritize visits to clusters if they are available, and alternatively, navigate towards the cell exhibiting the maximal information gain.

As the PDF of the source term represents the likeliness of the source presence in each cell given the current observations, it stands as the most straightforward and computationally efficient way to convey the information contained within each cell. During each iteration k, the probability $p\left(\mathbf{\Theta} \mid D_{1:k}\right)$ is normalized based on the min-max value, and only the cells with normalized probability exceeding a given threshold are retained. The threshold th is dynamically tuned based on the entropy of the PDF, which is defined as follows:

$$th = 1 - \mathbb{E}\left[log(p\left(\mathbf{\Theta}\right)\right]/\zeta \quad \text{with} \quad \zeta \geq \mathbb{E}\left[log(g\left(\mathbf{\Theta}\right)\right] \quad (2)$$

The th remains a positive value, with ζ larger than the entropy of the uniform distribution $g(\cdot)$ across all $\mathbf{\Theta}$. At the beginning of the task, no information is available for the estimation; thus $p\left(\mathbf{\Theta}\right) = g\left(\mathbf{\Theta}\right)$. The navigation algorithm favors at the beginning a more exploratory strategy, considering a wider range of cells. As the level of uncertainty in estimation reduces, the navigation shifts towards a more exploitative strategy, focusing solely on cells with a relatively high source-containing likelihood. The term ζ is utilized to establish a trade-off between exploration and exploitation.

b. Scanning of informative regions - Following the definition of the informative region, a cluster prioritization strategy is introduced. Given the knowledge of the gas dispersion model, a physical sample at every cell in a cluster is not necessary. To maximize the spatial coverage, a rough scan of a cluster is required. In this study, a simplified scanning strategy is employed. When clusters are present, a rectangle bounding box is computed for each cluster. The candidate movement is then defined as directing the robot towards the farthest vertex of each bounding box, which is considered as the rough scan of the cluster. The cluster resulting in the shortest traveling distance (to its farthest vertex) is selected to minimize unnecessary back-and-forth movements.

III. Simulation Experiments

This section presents simulation experiments supporting a *sense-in-motion* strategy. Additionally, we compare the performance of KLD- and belief-clustering-based IPP approaches.

A. Experimental Setup

We evaluated the different strategies in six diverse environments of 13×4 m areas, whose maps and coordinates are shown in Fig. 2. The testing maps were carefully hand-picked to guarantee the generality of the results. Maps 1 to 4 were

retained from our previous work [32], as the performance of DDPM had already been systematically evaluated in simulation and physical reality. We have introduced Map 5, as it presents a more challenging scenario due to the larger size of the obstacles in comparison to those used in the training dataset of the DDPM. In addition to these five maps, including obstacles representative of built environments, we have incorporated an obstacle-free environment, Map 0, which allows us to use the analytical plume model GPM instead, to demonstrate that the advantages of our method are not dependent on the chosen plume model. The simulations are conducted using Webots, an open-source, high-fidelity robotic simulator [35], augmented with a gas dispersion plugin [36] based on a filament-based model [37]. Each environmental configuration is evaluated ten times using a simulated Khepera IV robot. To ensure a rigorous and fair evaluation of the strategies, the initial position of the robot is randomized in the arena. The source position remains in the upwind edge, with the y-coordinate set randomly. The robot's maximal speed is set as 0.2 m/s. The minimal sampling period of the simulated gas sensor is 64 ms, corresponding to the simulated timestep. Given the communication bandwidth available on real robots (see Section IV-A), we opted to keep only one gas measurement out of ten in simulation to maintain as close as possible consistency with the physical experiments.

The performance of each strategy is evaluated in terms of source localization error, which is the Euclidean distance between the estimated and true source position. For each iteration, the robot updates the belief of the source terms and selects the next goal position. Thus, the required number of iterations for STE convergence is also evaluated to assess the system's efficiency.

B. Evaluation of Stop-sense-go and Its Arguments

Here, we present results from carefully designed experiments to assess the significance of the previously explained arguments in favor of a *stop-sense-go* strategy.

1) Evaluation of Argument I - Plume dynamics: To assess the impact of using immediate rather than time-averaged readings in a patchy plume, we compare the system performance using an *ideal* sensor for both *stop-sense-go* and *visit-sense-go* strategies. Fig. 3 reveals that both strategies when provided with ideal gas measurements exhibit comparable localization errors. However, *visit-sense-go* requires slightly more iterations to converge. This can be attributed to the fact that the probabilistic formulation inherently incorporates the potential mismatch between the physical gas dispersion

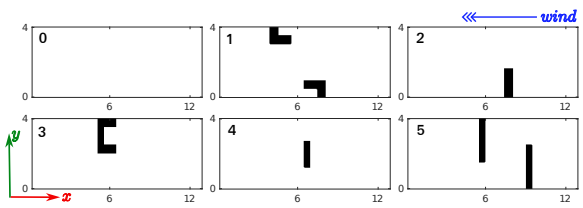

Fig. 2: The obstacle configuration of test maps.

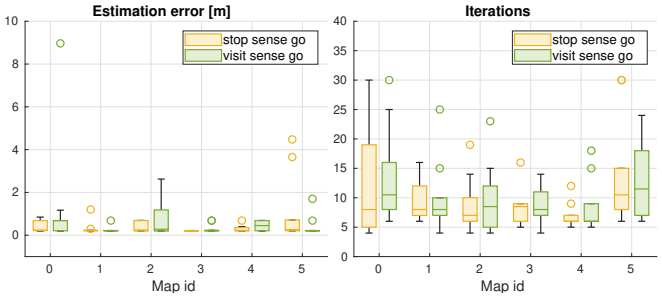

Fig. 3: Comparison between *stop-sense-go* and *visit-sense-go* with an ideal gas sensor and IPP based on KLD.

and the underlying model, which is represented by the term σ_M in the likelihood calculation, as shown in Eq. 1. The degradation in sample accuracy raises the required number of iterations to reach a confident estimation.

In conclusion, these findings indicate that, despite the time-averaged property of the plume models, instantaneous readings capture sufficient features of the plume for GSL.

2) Evaluation of Argument II - Sensor properties: To evaluate the influence of the MOX sensor's dynamic properties on GSL tasks, the *stop-sense-go* and *visit-sense-go* strategies are compared using a *MOX* sensor. The response and recovery phases of a MOX sensor, are simulated as two first-order systems, as in [5] [38]. The parameters of the simulated MOX sensor are calibrated to match the actual deployed sensor in reality (MiCS-5521), with a response and recovery time of 2.04 s and 4.57 s, respectively. The results presented in Fig. 4 show that the *stop-sense-go* approach exhibits comparable localization accuracy as those obtained with an ideal gas sensor. However, the *visit-sense-go* strategy with a MOX sensor is not able to localize the source within the maximum iteration number, which is consistent with the findings in [18] [11]. This can be explained by the fact that the *stop-sense-go* strategy enables the MOX sensor to respond to the actual concentration through the prolonged stop phase. However, in the case of the *visit-sense-go*, the immediate reaction of the MOX sensor deviates from the actual concentration level, resulting in estimation divergence in most scenarios.

In summary, the above findings suggest that the slow dynamics of the MOX sensor further diminish the sensing quality in the case of a too brief stop at the sampling point, leading to failures in GSL tasks.

C. Evaluation of Sense-in-motion

Inspired by model-free GSL algorithms, we decided to further investigate the impact of taking all measurements into account, including those acquired during motion with a MOX sensor. Surprisingly, as shown in Fig. 4, the *sense-in-motion* strategy achieves comparable results to the *stop-sense-go* strategy in terms of localization error, with a significantly lower amount of iterations required. This finding contradicts the intuition that an increased quantity of noisy measurements would make the estimation algorithm further diverge. Several factors can explain this result. Firstly, the *sense-in-motion* method incorporates more data between sampling

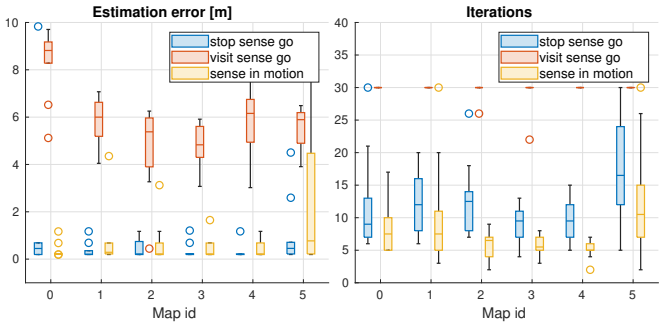

Fig. 4: Comparison of *stop-sense-go*, *visit-sense-go* and *sense-in-motion* with a MOX sensor and IPP based on KLD.

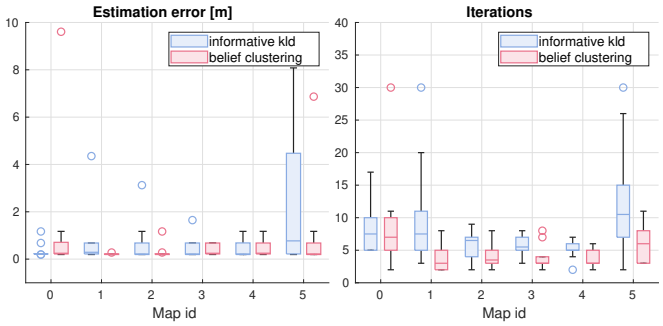

Fig. 5: Comparison of KLD versus belief-clustering based IPP approaches with *sense-in-motion* and a MOX sensor.

points, a spatial aggregation process that appears to offer similar advantages to the temporal averaging process in the *stop-sense-go* method. Secondly, although a MOX sensor cannot provide accurate measurements at the sampling points in motion, it is nevertheless capable of providing a delayed response faithful to the concentration in the proximity area. Thus, *sense-in-motion* increases the probability of capturing the existence of gas particles in a region. Thirdly, when considering solely one measurement at the sampling point, the outcome of the IPP has a substantial impact on the efficiency of the algorithm. The effectiveness of IPP is tightly related to the estimation results. In the case of the *visit-sense-go* strategy, when the estimation is off, the robot cannot be guided to appropriate positions, resulting in an increased failure rate. However, with a *sense-in-motion* strategy, the measurements obtained during motion leading to a potentially suboptimal goal position are still taken into account, partially mitigating the impact associated to a single measurement at suboptimal positions. Regarding the required iterations, as more samples are accessible at each iteration, the convergence of the estimation algorithm is accelerated.

In conclusion, even though the quality of gas sensing is degraded without a sufficient stop duration while sampling, this factor can be mitigated through the adoption of a *sense-in-motion* approach.

D. Performance Across Maps

Overall, the relative performance differences among the three strategies remain consistent across all the maps, with or without obstacles. Meanwhile, some noteworthy observations warrant discussion. A reduced estimation accuracy is observed in Map 5 with the MOX sensor. Given the fact that Map 5 is featured with more challenging obstacles, it can be treated as an unseen environment for the DDPM, hence degrading the quality of plume modeling. When this factor is combined with the MOX sensor, there is a noticeable increase in the variability of the failure rate. This finding provides additional evidence for the correlation between the quality of sensing/modeling and the estimation convergence.

E. Evaluation of IPP Based on Belief Clustering

The comparison of the *sense-in-motion* strategy using a MOX sensor with the informative KLD and the belief clustering methods is shown in Fig. 5. The belief clustering method achieves comparable localization error to KLD planning in obstacle-free and built environments (Map 1 to 4) while outperforming it in the challenging scenario (Map 5). The observed improvement of belief clustering planning can be explained by its reliance on the selection of informative cells based on a percentage threshold rather than being contingent upon exact values. This characteristic reduces the dependence of planning performance on the accuracy of estimation, allowing the robot to navigate toward important locations more robustly. Furthermore, the exploratory behavior exhibited during the early stage of the belief-clustering strategy serves to enhance the spatial coverage of gas samples, hence increasing the chance of capturing the presence of the gas plume. This, in turn, leads to a reduction of the necessary iterations.

IV. Physical Experiments

This section presents the validation of the proposed methods through physical experiments. The performance of the belief-clustering-based planning algorithm with the *sense-in-motion* strategy was benchmarked with the informative KLD-based planning algorithm with the *stop-sense-go* strategy. In the following text, we will refer to these methods as *cluster-motion-sense* and *KLD-stop-sense*, respectively.

A. Experimental Setup

The experiments were carried out within our wind tunnel facility, as shown in Fig. 7, ensuring consistent testing conditions throughout multiple runs. The wind tunnel provides a volume of $18 \times 4 \times 1.9$ m, and is equipped with a Motion Capture System (MCS), which offers accurate localization information to the robots. The wind speed was kept at 0.75 m/s throughout all the experiments. Three maps were selected to be reproduced in reality, namely Maps 2, 4 and 5. For each map, nine experiments were conducted, with the source's x position held constant in an upwind position, while y is selected within a predefined set, namely $S_y = \{1 \text{ m}, 2 \text{ m}, 3 \text{ m}\}$ to cover the y-axis broadly. A Khepera IV robot, equipped with a gas sensing module composed of a MiCS-5521 sensor, sampled at 10 Hz, was used as the mobile robotic platform. The maximal speed of the robot was set as 0.27 m/s. The STE algorithm was executed on a laptop (Intel Core i7-12700H). After each iteration, a new goal position was sent to the robot. The robot navigated

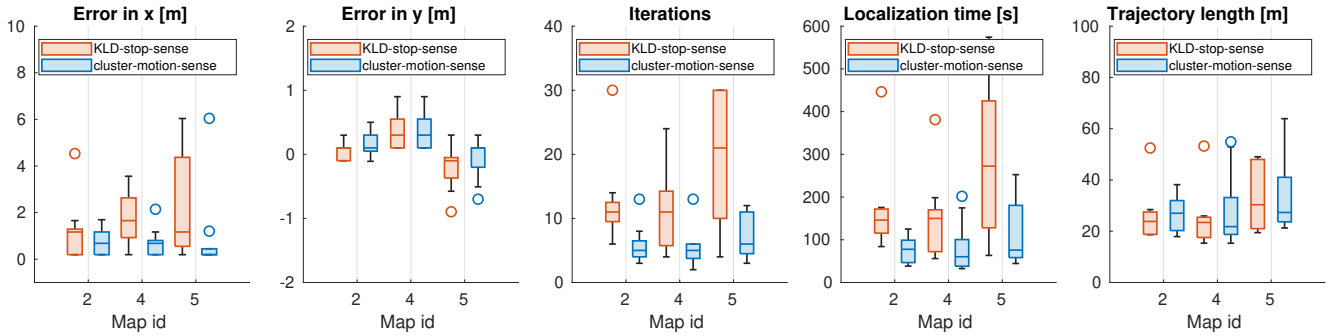

Fig. 6: Results of physical experiments in the wind tunnel.

to each goal point, collected gas samples, and transmitted them back to the laptop. Due to the limited communication bandwidth, while sampling continuously, one out of eight samples was retained and used for the estimation process.

B. Results and Discussion

The results of the physical experiments can be seen in Fig. 6. In terms of metrics, besides the localization error on the X- and Y-axis and the required iterations, the time to localize the source and the traveling length have been also considered. The localization time is the total time required to complete a single trial, including the time for navigation, sampling, and STE computation. We have tested the performance of *KLD-stop-sense* in Maps 2 and 4 in our previous work [32], which revealed a satisfactory performance in Map 2 but an increased estimation error in Map 4. We repeated the experiments, and similar results were observed here. The observed outcome was likely due to the fact that Map 4 exhibits a more transitory scenario compared to Map 2. This can be attributed to the presence of a rectangular object positioned in the center, which potentially leads to the generation of a Kármán vortex street [39] behind the obstacle. However, capturing this phenomenon in the plume model is challenging because of its time-average nature. A degradation in performance of the *KLD-stop-sense* method is observed in Map 5, consistently with the simulation results, given the increased challenge in obstacle configuration. Compared to the *KLD-stop-sense* strategy, the *cluster-motion-sense* achieved a similar performance in Map 2 while demonstrating superior performance in Maps 4 and 5. The observed results confirm those obtained in simulation: the *cluster-motion-sense* method achieves better localization accuracy in case of a discrepancy between the gas plume model and reality. This is achieved by obtaining more gas samples with the *sense-in-motion* strategy and expanding the spatial coverage with the belief-clustering method.

Fig. 7: The experimental setup in the wind tunnel.

In terms of the iterations, the *cluster-motion-sense* halved the necessary iterations for Map 2 and significantly decreased them for Maps 4 and 5. A similar trend can be observed in the localization time. This can be explained by the fact that the *sense-in-motion* behavior avoids stopping, which reduces sampling time. Additionally, the belief-clustering approach eliminates the PDF calculation for candidate goals, which decreases computing time. In terms of trajectory length, the results are similar across both methods. However, the *cluster-motion-sense* strategy exhibits a substantially longer traveling length per iteration. This limitation is brought by the more exploratory behavior of the belief-clustering strategy in the initial phase, which can be further improved.

V. Conclusion

The *sense-in-motion* strategies have been generally overlooked in existing model-based GSL algorithms due to the hard-to-model and noisy-to-sense nature of gas-sensing tasks. This study investigated the quantitative impact of such strategic choice in the context of GSL tasks. While we confirm that the gas sensing quality is degraded due to the limited raising and recovery speed of MOX sensors and the patchy property of the plume, we have shown that these challenges can be efficiently tackled by an increased amount of gas samples continuously gathered during navigation. Encouraged by the performance of continuous sampling in high-fidelity simulation, we further extended the IPP strategy from target-point sampling to target-region scanning. The performance of the approach was thoroughly assessed in both high-fidelity simulation and physical reality, in particular by considering different obstacle configurations and various starting points of the robot and placements of the source. When compared to a strategy based on informative KLD and measurement stops, our novel approach combining *sense-in-motion* and belief-clustering-based IPP reached a comparable level of performance in terms of localization error and a superior one in terms of time and number of iterations needed to localize the source. Such results are encouraging us to further investigate GSL approaches leveraging a *sense-in-motion* strategy.

REFERENCES

[1] T. Jing, Q. Meng, and H. Ishida, "Recent Progress and Trend of Robot Odor Source Localization," *IEEJ Transactions on Electrical and Electronic Engineering*, vol. 16, no. 7, pp. 938–953, July 2021, number: 7. [Online]. Available: https://onlinelibrary.wiley.com/doi/10.1002/tee.23364

[2] M. Rossi and D. Brunelli, "Gas Sensing on Unmanned Vehicles: Challenges and Opportunities," in *New Generation of CAS*. Genova, Italy: IEEE, Sept. 2017, pp. 117–120. [Online]. Available: http://ieeexplore.ieee.org/document/8052283/

[3] N. Holmes and L. Morawska, "A review of dispersion modelling and its application to the dispersion of particles: An overview of different dispersion models available," *Atmospheric Environment*, vol. 40, no. 30, pp. 5902–5928, Sept. 2006. [Online]. Available: https://linkinghub.elsevier.com/retrieve/pii/S1352231006006339

[4] G. Kowadlo and R. A. Russell, "Using naïve physics for odor localization in a cluttered indoor environment," *Autonomous Robots*, vol. 20, no. 3, pp. 215–230, June 2006. [Online]. Available: http://link.springer.com/10.1007/s10514-006-7102-3

[5] J. G. Monroy, J. González-Jiménez, and J. L. Blanco, "Overcoming the Slow Recovery of MOX Gas Sensors through a System Modeling Approach," *Sensors*, vol. 12, no. 10, pp. 13 664–13 680, Oct. 2012. [Online]. Available: http://www.mdpi.com/1424-8220/12/10/13664

[6] T. Lochmatter, N. Heiniger, and A. Martinoli, "Localizing an Odor Source and Avoiding Obstacles: Experiments in a Wind Tunnel using Real Robots," in *AIP Conference Proceedings*. Brescia (Italy): AIP, 2009, pp. 69–72. [Online]. Available: http://aip.scitation.org/doi/abs/10.1063/1.3156629

[7] R. Rozas, J. Morales, and D. Vega, "Artificial smell detection for robotic navigation," in *Fifth International Conference on Advanced Robotics 'Robots in Unstructured Environments*, June 1991, pp. 1730–1733 vol.2.

[8] J. Burgués, V. Hernández, A. J. Lilienthal, and S. Marco, "Smelling nano aerial vehicle for gas source localization and mapping," *Sensors*, vol. 19, no. 3, p. 478, 2019.

[9] V. Hernandez Bennetts, A. J. Lilienthal, P. P. Neumann, and M. Trincavelli, "Mobile Robots for Localizing Gas Emission Sources on Landfill Sites: Is Bio-Inspiration the Way to Go?" *Frontiers in Neuroengineering*, vol. 4, 2012. [Online]. Available: http://journal.frontiersin.org/article/10.3389/fneng.2011.00020/abstract

[10] A. Keats, E. Yee, and F.-S. Lien, "Bayesian inference for source determination with applications to a complex urban environment," *Atmospheric Environment*, vol. 41, no. 3, pp. 465–479, Jan. 2007. [Online]. Available: https://linkinghub.elsevier.com/retrieve/pii/S1352231006008703

[11] E. Persson and D. A. Anisi, "A Comparative study of robotic gas source localization algorithms in industrial environments," *IFAC Proceedings Volumes*, vol. 44, no. 1, pp. 899–904, Jan. 2011. [Online]. Available: https://linkinghub.elsevier.com/retrieve/pii/S1474667016437237

[12] M. Park, S. An, J. Seo, and H. Oh, "Autonomous Source Search for UAVs Using Gaussian Mixture Model-Based Infotaxis: Algorithm and Flight Experiments," *IEEE Transactions on Aerospace and Electronic Systems*, vol. 57, no. 6, pp. 4238–4254, Dec. 2021. [Online]. Available: https://ieeexplore.ieee.org/document/9492004/

[13] C. Rhodes, C. Liu, and W.-H. Chen, "Autonomous Source Term Estimation in Unknown Environments: From a Dual Control Concept to UAV Deployment," *IEEE Robotics and Automation Letters*, vol. 7, no. 2, pp. 2274–2281, Apr. 2022. [Online]. Available: https://ieeexplore.ieee.org/document/9684970/

[14] F. Rahbar, A. Marjovi, and A. Martinoli, "An algorithm for odor source localization based on source term estimation," in *IEEE International Conference on Robotics and Automation*, 2019, pp. 973–979. [Online]. Available: https://ieeexplore.ieee.org/document/8793784/

[15] P. Ojeda, J. Monroy, and J. González-Jiménez, "Information-Driven Gas Source Localization Exploiting Gas and Wind Local Measurements for Autonomous Mobile Robots," *IEEE Robotics and Automation Letters*, vol. 6, no. 2, pp. 1320–1326, Apr. 2021. [Online]. Available: https://ieeexplore.ieee.org/document/9347683/

[16] T. Wiedemann, D. Shutin, and A. J. Lilienthal, "Model-based gas source localization strategy for a cooperative multi-robot system—A probabilistic approach and experimental validation incorporating physical knowledge and model uncertainties," *Robotics and Autonomous Systems*, vol. 118, pp. 66–79, Aug. 2019. [Online]. Available: https://linkinghub.elsevier.com/retrieve/pii/S0921889018303816

[17] Y. Ji, Y. Zhao, B. Chen, Z. Zhu, Y. Liu, H. Zhu, and S. Qiu, "Source searching in unknown obstructed environments through source estimation, target determination, and path planning," *Building and Environment*, vol. 221, p. 109266, Aug. 2022. [Online]. Available: https://linkinghub.elsevier.com/retrieve/pii/S0360132322005017

[18] P. Ojeda, J. Monroy, and J. González-Jiménez, "Experimental Analysis of the Impact of Sensor Response Time on Robotic Gas Source Localization," in *IEEE International Symposium on Olfaction and Electronic Nose*. Aveiro, Portugal: IEEE, May 2022, pp. 1–3. [Online]. Available: https://ieeexplore.ieee.org/document/9789652/

[19] J. Burgués, V. Hernández, A. Lilienthal, and S. Marco, "Smelling Nano Aerial Vehicle for Gas Source Localization and Mapping," *Sensors*, vol. 19, no. 3, p. 478, Jan. 2019, number: 3. [Online]. Available: https://www.mdpi.com/1424-8220/19/3/478

[20] C. Ercolani and A. Martinoli, "3D odor source localization using a micro aerial vehicle: System design and performance evaluation," in *2020 IEEE/RSJ International Conference on Intelligent Robots and Systems*, 2020, pp. 6194–6200.

[21] J. G. Monroy and J. González-Jiménez, "Gas classification in motion: An experimental analysis," *Sensors and Actuators B: Chemical*, vol. 240, pp. 1205–1215, Mar. 2017. [Online]. Available: https://linkinghub.elsevier.com/retrieve/pii/S0925400516314307

[22] A. Lilienthal, A. Zell, M. Wandel, and U. Weimar, "Sensing odour sources in indoor environments without a constant airflow by a mobile robot," in *IEEE International Conference on Robotics and Automation*, vol. 4. Seoul, South Korea: IEEE, 2001, pp. 4005–4010. [Online]. Available: http://ieeexplore.ieee.org/document/933243/

[23] C. Ercolani, L. Tang, and A. Martinoli, "GaSLAM: An Algorithm for Simultaneous Gas Source Localization and Gas Distribution Mapping in 3D," in *IEEE/RSJ International Conference on Intelligent Robots and Systems*. Kyoto, Japan: IEEE, Oct. 2022, pp. 333–340. [Online]. Available: https://ieeexplore.ieee.org/document/9981976/

[24] M. Reggente and A. J. Lilienthal, "The 3D-Kernel DM+V/W algorithm: Using wind information in three dimensional gas distribution modelling with a mobile robot," in *IEEE Sensors*. Kona, HI: IEEE, Nov. 2010, pp. 999–1004. [Online]. Available: http://ieeexplore.ieee.org/document/5690924/

[25] M. Hutchinson, H. Oh, and W.-H. Chen, "A review of source term estimation methods for atmospheric dispersion events using static or mobile sensors," *Information Fusion*, vol. 36, pp. 130–148, July 2017. [Online]. Available: https://linkinghub.elsevier.com/retrieve/pii/S156625351630152X

[26] M. Vergassola, E. Villermaux, and B. I. Shraiman, "'Infotaxis' as a strategy for searching without gradients," *Nature*, vol. 445, no. 7126, pp. 406–409, Jan. 2007. [Online]. Available: http://www.nature.com/articles/nature05464

[27] J. R. Bourne, M. N. Goodell, X. He, J. A. Steiner, and K. K. Leang, "Decentralized Multi-agent information-theoretic control for target estimation and localization: finding gas leaks," *The International Journal of Robotics Research*, vol. 39, no. 13, pp. 1525–1548, Nov. 2020. [Online]. Available: http://journals.sagepub.com/doi/10.1177/0278364920957090

[28] M. Hutchinson, C. Liu, and W. Chen, "Source term estimation of a hazardous airborne release using an unmanned aerial vehicle," *Journal of Field Robotics*, vol. 36, no. 4, pp. 797–817, June 2019. [Online]. Available: https://onlinelibrary.wiley.com/doi/10.1002/rob.21844

[29] P. Ojeda, J. Monroy, and J. González-Jiménez, "Robotic Gas Source Localization with Probabilistic Mapping and Online Dispersion Simulation," *arXiv:2004.08826 [physics]*, no. 23, 2023. [Online]. Available: https://arxiv.org/pdf/2304.08879.pdf

[30] C. Wang, L. Yin, L. Zhang, D. Xiang, and R. Gao, "Metal Oxide Gas Sensors: Sensitivity and Influencing Factors," *Sensors*, vol. 10, no. 3, pp. 2088–2106, Mar. 2010. [Online]. Available: http://www.mdpi.com/1424-8220/10/3/2088

[31] F. Rahbar and A. Martinoli, "A Distributed Source Term Estimation Algorithm for Multi-Robot Systems," in *IEEE International Conference on Robotics and Automation*. Paris, France: IEEE, May 2020, pp. 5604–5610. [Online]. Available: https://ieeexplore.ieee.org/document/9196959/

[32] W. Jin, F. Rahbar, C. Ercolani, and A. Martinoli, "Towards Efficient Gas Leak Detection in Built Environments: Data-Driven Plume Modeling for Gas Sensing Robots," in *IEEE International Conference on Robotics and Automation*. London, United Kingdom:

IEEE, May 2023, pp. 7749–7755. [Online]. Available: https://ieeexplore.ieee.org/document/10160816/

[33] S. Kullback and R. A. Leibler, "On information and sufficiency," *The Annals of Mathematical Statistics*, vol. 22, no. 1, pp. 79–86, 1951.

[34] M. Ester, H.-P. Kriegel, J. Sander, X. Xu, *et al.*, "A density-based algorithm for discovering clusters in large spatial databases with noise." in *kdd*, vol. 96, no. 34, 1996, pp. 226–231.

[35] O. Michel, "Cyberbotics Ltd. Webots™: professional mobile robot simulation," *International Journal of Advanced Robotic Systems*, vol. 1, no. 1, pp. 39–42, 2004.

[36] "Webots Odor Simulation/Model - Wikibooks, open books for an open world." [Online]. Available: https://en.wikibooks.org/wiki/Webots_Odor_Simulation/Model

[37] J. A. Farrell, J. Murlis, X. Long, W. Li, and R. Carde, "Filament-Based Atmospheric Dispersion Model to Achieve Short Time-Scale Structure of Odor Plumes," Defense Technical Information Center, Fort Belvoir, VA, Tech. Rep., Jan. 2002. [Online]. Available: http://www.dtic.mil/docs/citations/ADA399832

[38] J. Monroy, V. Hernandez-Bennetts, H. Fan, A. Lilienthal, and J. González-Jiménez, "GADEN: A 3D Gas Dispersion Simulator for Mobile Robot Olfaction in Realistic Environments," *Sensors*, vol. 17, no. 7, p. 1479, June 2017, number: 7. [Online]. Available: http://www.mdpi.com/1424-8220/17/7/1479

[39] R. Wille, "Kármán vortex streets," ser. Advances in Applied Mechanics, H. Dryden, T. von Kármán, G. Kuerti, F. van den Dungen, L. Howarth, and J. Pérès, Eds. Elsevier, 1960, vol. 6, pp. 273–287. [Online]. Available: https://www.sciencedirect.com/science/article/pii/S0065215608701133